PHYSICAL REVIEW B VOLUME 9, NUMBER 4 15 FEBRUARY 1974

Resistivity of nearly magnetic metals at high temperatures: Application to neptunium and plutonium*

R. Jullien, M. T. Béal-Monod, and B. Coqblin
Laboratoire de Physique des Solides,† Université Paris-Sud, 91405 Orsay, France
(Received 16 July 1973)

It is shown that, in nearly magnetic metals, taking into account the temperature depndence of the Stoner susceptibility makes the electron-paramagnon electrical resistivity depart from the usual low-temperature T^2 and T power laws at temperatures higher than the spin-fluctuation one. A high-temperature plateau is expected and a maximum may arise at lower temperatures depending on two parameters: the Stoner exchange-enhancement factor and the relative values of the Fermi wavelengths of the conduction and the interacting electrons. Possible fits are presented for the resistivities of palladium, neptunium, and plutonium and the case of strongly exchange-enhanced actinide compounds is also discussed.

I. INTRODUCTION

It is well known that the spin-fluctuation resistivity in nearly magnetic metals and alloys exhibits an enhanced T^2 law at very low temperature.[1] It has also been shown that this behavior is followed at higher temperatures by a linear T law.[2] These T^2 and T laws are effectively encountered at low temperatures in nearly magnetic alloys (Pi-Ni[1]) as well as in strongly enhanced pure metals (Pd,[1] Np,[3] Pu[3]). However, it is clear experimentally that, in the spin-fluctuation systems, either in alloys such as RhFe,[4] IrFe,[5] PtFe,[6] PdCo,[7] and PdV,[8] or in pure metals, the resistivity departs from a T law at higher temperatures with a negative curvature and thus bends over towards the T axis. This high-temperature behavior cannot be accounted for by the above theories[1,2] as they stand, since they do not take into account the temperature variation of the spin-correlation function which can no longer be forgotten at high temperature. Kaiser and Doniach[2] have tried to take care of that point using a low-temperature expansion of the susceptibility; this was a first improvement, but it is not sufficient to account for the whole temperature variation of the resistivity so that they were obliged to choose huge exchange-enhancement factors in order to fit the experimental data on dilute alloys. In the case of local enhancement, Rivier and Zlatič[9] have recently proposed to treat the high-temperature resistivity the same way they treated the Kondo problem,[10] so that they infer that the resistivity should reach its unitary limit at high temperatures.

We study here the case of pure metals with a uniform enhancement; we show that taking into account the full temperature dependence of the paramagnon susceptibility can account for the behavior of the resistivity on the whole temperature range: i.e., we explain the observed negative curvature at high temperature and the same formula reduces at low temperature to the usual results.[1,2] A preliminary account of that work has been already given elsewhere.[11] The resistivities of the well-known exchange-enhanced metals palladium[12] and platinium[13] begin to depart from the linear law roughly at room temperature. The resistivity of the nearly magnetic α-phase of cerium seems also to depart from a linear law above 70 K,[14] but the resistivity data on α-cerium are presently controversial.[14–17] The most striking effects are in fact observed on the high-temperature resistivities of neptunium and plutonium. The resistivity of neptunium presents a large T^2 term at low temperatures,[3] departs from a T law at roughly 80 K, then saturates and remains almost constant between 300 and 500 K.[18] The resistivity of plutonium behaves as T^2 and T at low temperatures,[3] departs from a linear law at roughly 40 K to reach a maximum or order 160 $\mu\Omega$cm at roughly 100 K and then decreases slowly up to 600 K[18–22]; the resistivity decrease arises in all phases of plutonium,[18,20] as well as in many plutonium-based alloys.[21–25] Several explanations for the temperature variation of the Pu resistivity have been proposed previously, but most of them have been ruled out by experiments (see the review article by Arko *et al.*[3]). Presently the spin-fluctuation model seems the best one to account for the different properties of Pu[3,26]; within that framework Arko *et al.*[3] and Doniach,[26] in order to explain the high-temperature resistivity behavior of Pu, have proposed that the 5f bands, hybridized at low temperatures, becomes narrower and "dehybridized" at high temperatures, which would lead to a high-temperature saturation. We will show that the high-temperature plateau for the resistivity can be found without invoking that dehybridization effect, which may well be present, though.

II. TEMPERATURE DEPENDENCE OF PARAMAGNON PROPAGATOR

A. Model and approximations

We use the classical paramagnon model: the conduction electrons (labeled by the index c) of one broad band are scattered by large spin fluctuations formed by the strongly interacting electrons (labeled by the index i) of a second very narrow band. We assume that only the c electrons are free and contribute to the resistivity and also that the Fermi temperatures of the two bands are very different: the Fermi temperature T_{Fc} of the conduction band is assumed to be much larger than all the usual temperatures, but the Fermi temperature T_{Fi} of the interacting band can be within the usual temperature range.

We follow the Kaiser-Doniach[2] notation for the formal expression of the electron-paramagnon resistivity:

$$\rho = \frac{\rho_0}{T} \int_0^{2k_{Fc}} \frac{q^3 dq}{k_{Fc}^4} \int_0^{\infty} 2\,\mathrm{Im}\chi(q,\omega,T) \times \frac{\omega d\omega}{(e^{\omega/T}-1)(1-e^{-\omega/T})}, \quad (1)$$

with

$$\rho_0 = \left(\frac{JN(\epsilon_{F_c})}{4}\right)^2 \frac{m_c}{n_c e^2 \tau_{F_c}} \frac{\nu}{n_c}. \quad (2)$$

$N(E_{F_c}) = m_c k_{Fc}/\hbar^2\pi^2\nu$ is the total density of states at the Fermi level for the two spin directions of the conduction band assumed to be parabolic; m_c, k_{Fc}, and n_c are, respectively, the effective mass, the Fermi wave vector, and the number of electrons per unit volume for the conduction band. $\hbar/\tau_{F_c} = \hbar^2 k_{Fc}^2/2m_c$ is the Fermi energy of conduction electrons. All these quantities for the conduction band are taken to be temperature independent, due to the assumed very high value of T_{F_c}. ν is the number of atoms per unit volume and J is the coupling constant between the electrons of the two bands. We use the units $k_B = \hbar = 1$.

The paramagnon propagator $\chi(q,\omega,T)$, i.e., the dynamic correlation function of the interacting electrons, is given in the random-phase approximation (RPA) by

$$\chi(q,\omega,T) = \frac{\chi^0(q,\omega,T)}{1 - I\chi^0(q,\omega,T)}, \quad (3)$$

where I is the phenomenological interaction between the i electrons and $\chi^0(q,\omega,T)$ is the dynamic susceptibility in absence of interaction, given as usual by

$$\chi^0(q,\omega,T) = \sum_{\vec{k}} \frac{f(\epsilon_{\vec{k}},T) - f(\epsilon_{\vec{k}+\vec{q}},T)}{\epsilon_{\vec{k}+\vec{q}} - \epsilon_{\vec{k}} - \omega - i\delta^+}. \quad (4)$$

δ^+ is a positive infinitesimal and $f(\epsilon_{\vec{k}},T)$ the Fermi-Dirac distribution

$$f(\epsilon_{\vec{k}},T) = \left[1 + \exp\left(\frac{\epsilon_{\vec{k}} - \epsilon_{Fi}(T)}{T}\right)\right]^{-1}. \quad (5)$$

$\chi^0(q,\omega,T)$ is defined for one spin direction, so that

$$\chi^0(0,0,0) = \tfrac{1}{2}N(\epsilon_{Fi}(0)), \quad (6)$$

where $N(\epsilon_{Fi}(0))$ designs the total density of states at the Fermi energy for $T=0$ for the two spin directions of the interacting band.

We recall the definition of the Stoner enhancement factor:

$$S = \frac{\chi(0,0,0)}{\chi^0(0,0,0)} = \frac{1}{1 - I\chi^0(0,0,0)} = \frac{1}{1-\bar{I}}. \quad (7)$$

The susceptibility $\chi^0(q,\omega,T)$ given by (4) depends on the temperature directly and through the temperature-dependent chemical potential $\epsilon_{Fi}(T)$ of the interacting i electrons. The thermal variation of the chemical potential $\epsilon_{Fi}(T)$ is implicitly given here by the conservation of the number of i electrons; i.e.,

$$2\sum_{\vec{k}} f(\epsilon_{\vec{k}},T) = n_i/\nu, \quad (8)$$

where n_i is the number of i electrons per unit volume.

The classical paramagnon theory,[1,2] which is restricted to a very-low-temperature study, does not need to consider the temperature variation of $\mathrm{Im}\chi(q,\omega,T)$ and takes its value $\mathrm{Im}\chi(q,\omega,0)$ at $T=0$ in the calculation of the resistivity. The improvement introduced here is to consider the total temperature dependence of the paramagnon propagator to derive the resistivity (1) in the whole temperature range. Assuming no thermal variation of I, the temperature dependence of the resistivity is formally given by Eqs. (1), (3), (4), and (8).

Before presenting the detailed calculations, let us comment on the approximations of the model:

(a) We deal here with pure nearly magnetic metals with uniform paramagnons. The extension to alloys with local paramagnons is not given here.

(b) We use the expression (3) and neglect the paramagnon corrections to χ^0, although at low temperatures already the ST^2 expansion of the Stoner susceptibility is known to be too weak to account for experiments on liquid He^3 and paramagnon corrections to χ^0 are necessary to get the correct S^2T^2 behavior observed experimentally.[27]

(c) We have assumed I to be temperature independent, but I is certainly weaker at high temperatures. However, since I appears as a phenomenological interaction in the paramagnon theory, it is difficult to infer its temperature dependence.

(d) We have assumed implicitely the same form for the free energy at high and low temperatures, leading to the same diagrammatic expansion of the RPA series (3) with (4). This is not obviously

true; in particular, particle-particle interactions negligible at low temperatures may be as important as particle-hole interactions at high temperatures. Furthermore the temperature dependence of the chemical potential of the i band obtained here in the usual way is not obviously the correct one: in particular, it is not obvious that it should remain insensitive to I. To take all of those features into account rigorously would be a difficult problem in itself and its effect on the resistivity behavior is not trivial.

(e) We have neglected the temperature dependence of the conduction-electron Fermi energy, which is assumed to be much larger that T_{Fi} and all usual temperatures. So, this model is especially valid for a good metal with a broad conduction band and a very narrow interacting band; it would have to be modified to apply to the case of semimetals such as Yb[28] or V_2O_3[29] which have very-small-T_{Fc} values.

(f) We have also neglected band-structure effects and calculated $\chi^0(q, \omega, T)$ for a parabolic i band. Moreover, in the case of actinides, we consider an sd conduction band and a localized f band and neglect the d-f hybridization, which is a huge approximation for actinides,[30] but again a rigorous treatment would have been much too intricate and no clear conclusion could have been drawn.

B. Calculation of $\chi(q,\omega,T)$

We compute here the susceptibility in the case of a parabolic i band; the energy $\epsilon_{\vec{k}}$ is given by

$$\epsilon_{\vec{k}} = k^2/2m_i \ , \tag{9}$$

where m_i is the effective mass of the i band. So, with (9), the expression (6) becomes

$$\chi^0(0,0,0) = \tfrac{1}{2}N(\epsilon_{Fi}(0)) = m_i k_{Fi}/2\pi^2\nu \ , \tag{10}$$

where

$$k_{Fi} = (3\pi^2 n_i)^{1/3} \tag{11}$$

is the Fermi wave vector of the i band at $T=0$.

The imaginary part of $\chi^0(q, \omega, T)$ is computed directly from (4), if we remember that

$$\lim_{\delta^+ \to 0} \mathrm{Im}\left(\frac{1}{\epsilon_{\vec{k}+\vec{q}} - \epsilon_{\vec{k}} - \omega - i\delta^+}\right) = \pi\delta(\epsilon_{\vec{k}+\vec{q}} - \epsilon_{\vec{k}} - \omega) \ . \tag{12}$$

Then, by transforming the sum over $\vec{k}$ of (4) into an integral over the modulus k of $\vec{k}$ and over $z = \cos\theta = \vec{k}\cdot\vec{q}/kq$, we obtain

$$\mathrm{Im}\chi^0(q, \omega, T) = \frac{1}{4\pi\nu}\int_{-1}^{+1} dz \int_0^\infty k^2 dk \times[f(\epsilon_{\vec{k}}, T) - f(\epsilon_{\vec{k}+\vec{q}}, T)] \times \delta\left(\frac{1}{m_i}(kqz + \tfrac{1}{2}q^2) - \omega\right) \ . \tag{13}$$

Performing the integration over z gives

$$\mathrm{Im}\chi^0(q, \omega, T) = \frac{m_i}{4\pi\nu q}\int_{|m_i\omega/q - q/2|}^\infty \times[f(\epsilon_k, T) - f(\epsilon_k + \omega, T)]k\,dk \ . \tag{14}$$

The imaginary part of $\chi^0(q, \omega, T)$ is obtained analytically after the integration over the energy. The imaginary part of the reduced susceptibility $\bar{\chi}^0(q, \omega, T) = \chi^0(q, \omega, T)/\chi^0(0,0,0)$ is finally given by

$$\mathrm{Im}\bar{\chi}^0(q, \omega, T) = \frac{\pi}{2}\frac{T}{v_{Fi}q} \times \ln\left[\frac{\exp(\omega/T) + \exp[\epsilon(q, \omega, T)/T]}{1 + \exp[\epsilon(q, \omega, T)/T]}\right] , \tag{15}$$

where $v_{Fi} = k_{Fi}/m_i$ is the Fermi velocity of the i electrons at $T=0$ and $\epsilon(q, \omega, T)$ is an energy defined by

$$\epsilon(q, \omega, T) = \frac{1}{2m_i}\left(\frac{m_i\omega}{q} + \frac{q}{2}\right)^2 - \epsilon_{Fi}(T) \ . \tag{16}$$

The thermal dependence of the Fermi energy $\epsilon_{Fi}(T)$ for the i band, which is defined by (8), can be written, in the present case of a parabolic band, as

$$\int_0^\infty \frac{\epsilon^{1/2}d\epsilon}{1 + \exp\{[\epsilon - \epsilon_{Fi}(T)]/T\}} = \tfrac{2}{3}[\epsilon_{Fi}(0)]^{3/2} \ , \tag{17}$$

with $\epsilon_{Fi}(0) = T_{Fi} = k^2_{Fi}/2m_i$.

Equation (17) gives a unique curve of $\epsilon_{Fi}(T)/\epsilon_{Fi}(0)$ vs T/T_{Fi}; this curve, obtained exactly by a numerical computation, is plotted on Fig. 1. Some expansions are valid for T tending to 0 or for T much larger than T_{Fi}, but to derive the variation of $\epsilon_{Fi}(T)$ for T close to T_{Fi}, we need the exact numerical computation shown on Fig. 1.

The variation of $\epsilon_{Fi}(T)$ is put in (15) and (16) to give the temperature dependence of $\mathrm{Im}\bar{\chi}^0(q, \omega, T)$. The real part of $\bar{\chi}^0(q, \omega, T)$ is given by the Kramers-Kronig relation:

$$\mathrm{Re}\bar{\chi}^0(q, \omega, T) = \frac{1}{\pi}\int_{-\infty}^{+\infty}\frac{\mathrm{Im}\bar{\chi}^0(q, \omega', T)d\omega'}{\omega' - \omega} = \frac{2}{\pi}\int_0^\infty \frac{\omega'\mathrm{Im}\bar{\chi}^0(q, \omega', T)d\omega'}{(\omega')^2 - \omega^2} \ . \tag{18}$$

Then the imaginary part of the reduced susceptibility $\bar{\chi}(q, \omega, T) = \chi(q, \omega, T)/\chi^0(0, 0, 0)$ is immediately obtained by (3); i.e.,

$$\mathrm{Im}\bar{\chi}(q, \omega, T) = \frac{\mathrm{Im}\bar{\chi}^0(q, \omega, T)}{[1 - \bar{I}\,\mathrm{Re}\bar{\chi}^0(q, \omega, T)]^2 + \bar{I}^2[\mathrm{Im}\bar{\chi}^0(q, \omega, T)]^2} \ , \tag{19}$$

where $\bar{I}$ is defined by (7) and (10).

Equation (19), with Eqs. (15)–(18), has been used to derive numerically $\mathrm{Im}\bar{\chi}(q, \omega, T)$.

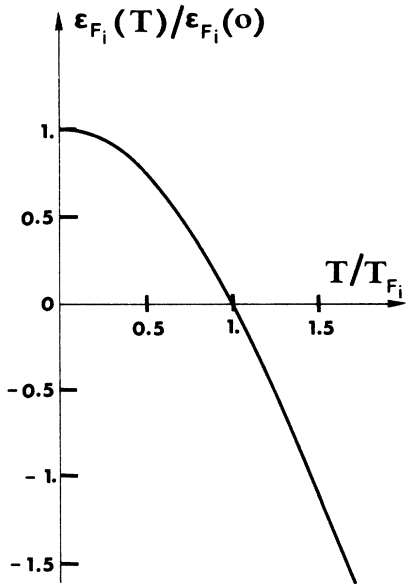

FIG. 1. Computed temperature variation of the chemical potential $\epsilon_{Fi}(T)/\epsilon_{Fi}(0)$ vs T/T_{Fi}.

C. Results for the susceptibility

The main results concerning the static susceptibilities $\chi^0(q, 0, T)$ and $\chi(q, 0, T)$, the dynamic susceptibility $\chi^0(q, \omega, T)$, and the imaginary part of the paramagnon susceptibility $\chi(q, \omega, T)$ are summarized below and described in the Figs. 2–5.

1. *Static susceptibility* $\chi^0(q,0,T)$

The reduced static susceptibility $\bar{\chi}^0(q, 0, T)$ which is real is given by (18) with $\omega = 0$ and is described by Figs. 2(a) and 2(b). Figure 2(a) shows the plot of $\bar{\chi}^0(q, 0, T)$ vs q/k_{Fi} for different values of T/T_{Fi}. At $T = 0$, we find back the classical curve[31]

$$\bar{\chi}^0(q, 0, 0) = \tfrac{1}{2}\left\{1 + \frac{k_{Fi}}{q}\left[1 - \left(\frac{q}{2k_{Fi}}\right)^2\right]\ln\left|\frac{1+q/2k_{Fi}}{1-q/2k_{Fi}}\right|\right\}. \tag{20}$$

The Kohn anomaly, which occurs at $q = 2k_{Fi}$ for $T = 0$, disappears when the temperature increases.

Figure 2(b) shows the plot of $\bar{\chi}(q, 0, T)$ vs T/T_{Fi} for different q/k_{Fi} values. At very large temperatures, a Curie law is obtained for the susceptibility:

$$[\chi^0(q, 0, T)]_{T\to\infty} = \frac{n_i}{2\nu}\frac{1}{T} \tag{21}$$

or, for the reduced susceptibility,

$$[\bar{\chi}^0(q, 0, T)]_{T\to\infty} = \tfrac{2}{3}T_{Fi}/T\ . \tag{22}$$

This limiting Curie law is plotted also in Fig. 2(b). The fact that the static susceptibility has to reach a Curie law at high temperatures is a very general result and is, in particular, independent of the i-band shape; the shape of the i band modifies only the way that the static susceptibility reaches the high-temperature Curie law.

2. *Static enhanced susceptibility* $\chi(q,0,T)$

The temperature dependence of the static enhanced susceptibility can be obtained directly from

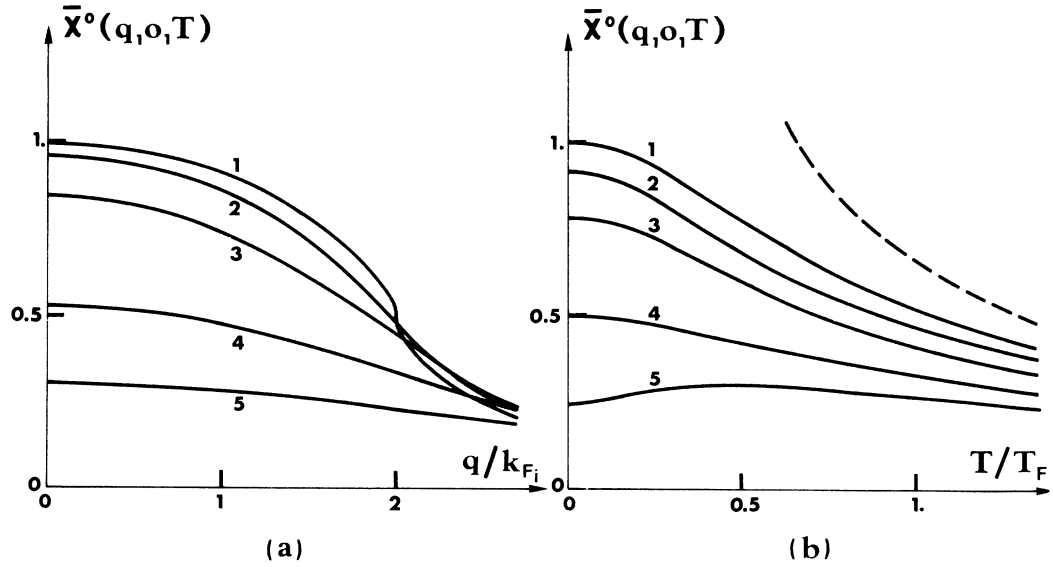

FIG. 2. Computed reduced static susceptibility $\bar{\chi}^0(q, 0, T)$: (a) versus q/k_{Fi} for different T/T_{Fi} values, the curves labeled 1, 2, 3, 4, 5 corresponding, respectively, to $T/T_{Fi} = 0$, 0.2, 0.4, 1; 2; (b) versus T/T_{Fi} for different q/k_{Fi} values, the curves labeled 1, 2, 3, 4, 5 corresponding, respectively to $q/k_{Fi} = 0$, 1, 1.5, 2, 2.5. The asymptotic high-temperature Curie law is given by the dashed line.

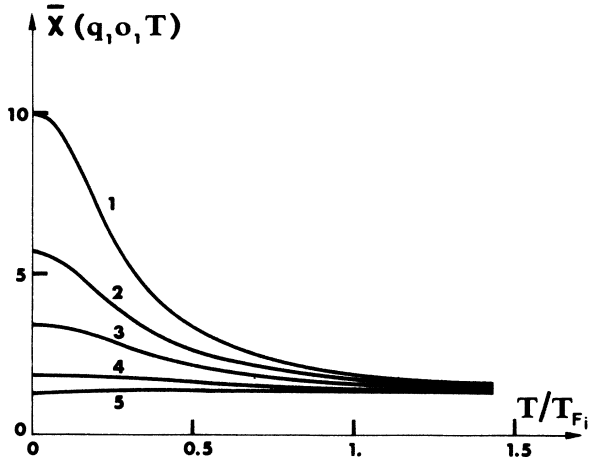

FIG. 3. Computed reduced enhanced static susceptibility $\bar{\chi}(q, 0, T)$ vs T/T_{Fi} for different q/k_{Fi} values, the curves labeled 1, 2, 3, 4, 5 corresponding, respectively, to $q/k_{Fi}=0$, 1, 1.5, 2, 2.5.

the static susceptibility without interaction [Fig. 2(b)] by use of (3), for a given value of the Stoner enhancement factor S. In Fig. 3, we have plotted the reduced static susceptibility $\bar{\chi}(q, 0, T)$ vs T/T_{Fi} in the case $S=10$ for the same values of q/k_{Fi} as those reported in Fig. 2(b). For $q=0$, the reduced static susceptibility starts from $T=0$ with a value equal to S and decreases very much with temperature in a temperature range around the spin-fluctuation temperature, defined here simply by $T_{sf}=T_{Fi}/S$; then it reaches the same high-temperature Curie law as $\chi^0(q, 0, T)$ given by the formula (21). The temperature decrease of $\chi(q, 0, T)$ becomes less important for large q values, due to the decrease of the product $I\chi^0$ with q.

3. *Dynamic susceptibility* $\chi^0(q,\omega,T)$

Figure 4 shows the plots of the real and the imaginary part of $\bar{\chi}^0(q, \omega, T)$ vs $\omega/v_{Fi}q$ for different q/k_{Fi} and T/T_{Fi} values. As it can be seen directly from (15) with $T\to 0$, one finds for $T=0$ the classical Lindhard function[31]:

$$\mathrm{Im}\bar{\chi}^0(q, \omega, 0)=\frac{\pi}{2}\frac{\omega}{v_{Fi}q}$$

$$\text{if } \left|\frac{\omega}{v_{Fi}q}\right| < \left|1-\frac{q}{2k_{Fi}}\right| \text{ and } \frac{q}{k_{Fi}}<2$$

$$=\frac{\pi}{4}\frac{k_{Fi}}{q}\left[1-\left(\frac{\omega}{v_{Fi}q}-\frac{q}{2k_{Fi}}\right)^2\right]$$

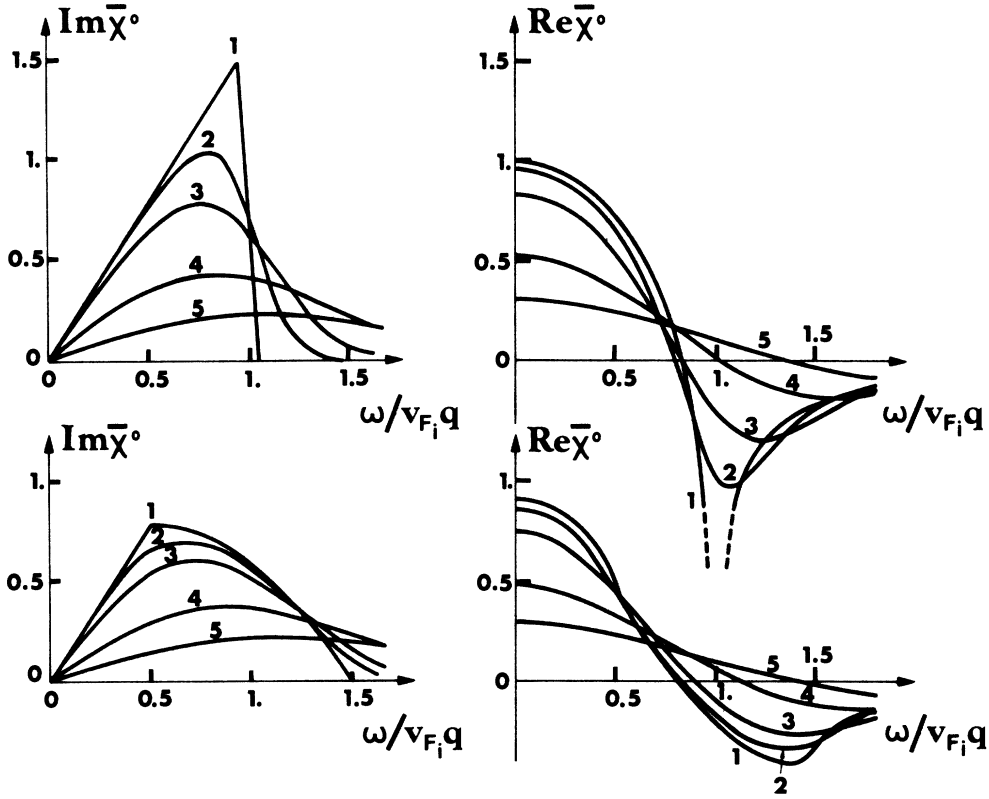

FIG. 4. Computed variations of the imaginary part and the real part of the dynamic reduced susceptibility $\bar{\chi}^0(q, \omega, T)$ vs $\omega/v_{Fi}q$ for two q/k_{Fi} values: $q/k_{Fi}=0.1$ (top of figure), $q/k_{Fi}=1$ (bottom of the figure); and for different T/T_{Fi} values, the curves labeled 1, 2, 3, 4, 5 corresponding, respectively, to $T/T_{Fi}=0$, 0.2, 0.4, 1, 2.

$$\text{if } \left|1-\frac{q}{2k_{Fi}}\right| < \left|\frac{\omega}{v_{Fi}q}\right| < \left|1+\frac{q}{2k_{Fi}}\right| = 0 \quad (23)$$

otherwise,

$$\mathrm{Re}\bar{\chi}^0(q,\omega,0) = \frac{1}{2}+\frac{1}{4}\frac{k_{Fi}}{q} \times\left\{\left[1-\left(\frac{\omega}{v_{Fi}q}+\frac{q}{2k_{Fi}}\right)^2\right] \times\ln\left|\frac{1+\omega/v_{Fi}q+q/2k_{Fi}}{1-\omega/v_{Fi}q-q/2k_{Fi}}\right| -\left[1-\left(\frac{\omega}{v_{Fi}q}-\frac{q}{2k_{Fi}}\right)^2\right] \times\ln\left|\frac{1+\omega/v_{Fi}q-q/2k_{Fi}}{1-\omega/v_{Fi}q+q/2k_{Fi}}\right|\right\} . \quad (24)$$

When the temperature increases, there is a general collapse of the $\bar{\chi}^0(q,\omega,T)$ curves and a broadening of the peaks; at very high temperatures, it results a small and smoothly varying susceptibility. The asymptotic form of these curves for $T\to\infty$ corresponds to the susceptibility of a Boltzmann gas, which is given by

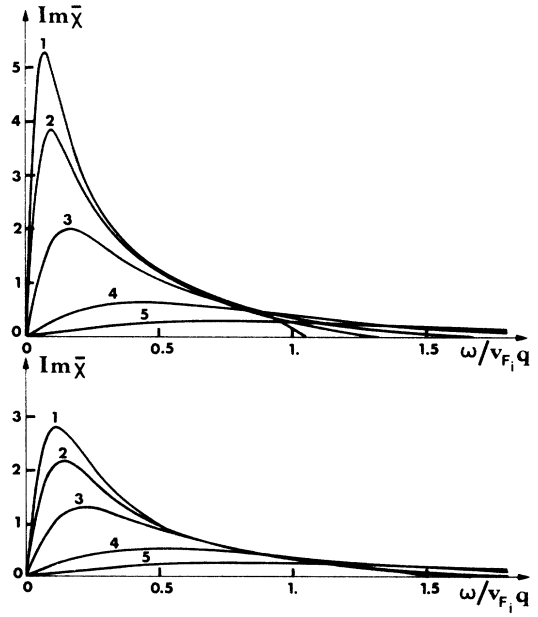

FIG. 5. Computed variation of the imaginary part of the reduced enhanced dynamic susceptibility $\bar{\chi}(q,\omega,T)$ vs $\omega/v_{Fi}q$ with a Stoner enhancement factor S equal to 10 for two q/k_{Fi} values: $q/k_{Fi}=0.1$ (top of the figure), $q/k_{Fi}=1$ (bottom of the figure); and for different T/T_{Fi} values, the curves laveled 1, 2, 3, 4, 5 corresponding, respectively, to $T/T_{Fi}=0$, 0.2, 0.4, 1, 2.

$$[\mathrm{Im}\bar{\chi}^0(q,\omega,T)]_{T\to\infty} = \frac{2}{3}\left(\frac{\pi}{2}\right)^{1/2}\frac{T_{Fi}}{T} \times\frac{(m_i\omega^2)^{1/2}}{Tq^2}\,e^{-m_i\omega^2/2Tq^2}, \quad (25)$$

$$[\mathrm{Re}\bar{\chi}^0(q,\omega,T)]_{T\to\infty} = \frac{2}{3}\frac{T_{Fi}}{T}\left(1-\frac{m_i\omega^2}{(\pi)^{1/2}Tq^2}\int_0^\infty\frac{e^{-t^2}dt}{m_i\omega^2/2Tq^2-t^2}\right) . \quad (26)$$

4. *Imaginary part of* $\chi(q,\omega,T)$

The imaginary part of $\bar{\chi}(q,\omega,T)$ is computed by the expression (19) as a function of $\mathrm{Im}\bar{\chi}^0(q,\omega,T)$ and $\mathrm{Re}\bar{\chi}^0(q,\omega,T)$, for a given $\bar{I}$ or S value. Figure 5 shows the plot of $\mathrm{Im}\bar{\chi}(q,\omega,T)$ vs $\omega/v_{Fi}q$ for different q/k_{Fi} and T/T_{Fi} values in the case of a large exchange-enhancement factor $S=10$.

One finds again, for $T=0$ and small q values, a peak centered at roughly $\omega/v_{Fi}q=1/S$ and with an intensity increasing with S. The effect of temperature is a general collapse of the $\mathrm{Im}\bar{\chi}(q,\omega,T)$ curves and a broadening of the peak as a direct consequence of what happens for $\bar{\chi}^0(q,\omega,T)$. For T of order T_{Fi}, there is no longer any peak: $\mathrm{Im}\bar{\chi}(q,\omega,T)$ is very small and flat. So, the effect of temperature is essentially to destroy the peak characteristic of paramagnons and thus one can no longer speak of enhanced spin fluctuations in the usual sense at high temperature. This is reasonable since the concept of paramagnon is linked to the one of quasiparticles in the Fermi-liquid theory which applies only at low temperature, so that this concept should become irrelevant at very high temperature.

III. PARAMAGNON RESISTIVITY

A. Resistivity saturation at high temperatures

Before presenting the calculation of the resistivity for the whole temperature range, let us first derive its asymptotic form at high temperatures.

The expansion of the exponentials in (1) for $T\to\infty$ leads to

$$\rho_{T\to\infty}\simeq\rho_0 T\int_0^{2k_{Fc}}\frac{q^3dq}{k_{Fc}^4}\int_0^\infty\frac{2\mathrm{Im}\chi(q,\omega,T)}{\omega}d\omega . \quad (27)$$

Using the Kramers-Kronig relation,[32] we can write

$$\int_0^\infty\frac{2\mathrm{Im}\chi(q,\omega,T)}{\omega}d\omega=\pi\mathrm{Re}\chi(q,0,T)=\pi\chi(q,0,T) , \quad (28)$$

so that the asymptotic form of ρ becomes

$$\rho_{T\to\infty}\simeq\pi\rho_0 T\int_0^{2k_{Fc}}\frac{\chi^0(q,0,T)}{1-I\chi^0(q,0,T)}\frac{q^3dq}{k_{Fc}^4} . \quad (29)$$

We see immediately from (29) that if we do not take into account the temperature dependence of $\chi^0(q,\omega,T)$, the asymptotic form of ρ is linear in

temperature, as previously found.[6] On the contrary, if we take into account the thermal dependence of $\chi^0(q, \omega, T)$, the limit for $T \to \infty$ of the static susceptibility is given by (21) and the resistivity tends to a constant value at high temperatures. By use of (21) and (29), the high-temperature limit ρ_∞ of ρ is equal to

$$\rho_\infty = \frac{\pi}{2} \rho_0 \frac{n_i}{\nu} \int_0^{2k_{Fc}} \frac{q^3 dq}{k_{Fc}^4} = 2\pi\rho_0 \frac{n_i}{\nu} \tag{30}$$

or, with (2),

$$\rho_\infty = \frac{\pi}{8} [JN(\epsilon_{F_c})]^2 \frac{m_c}{n_c e^2 \tau_{Fc}} \frac{n_i}{n_c} . \tag{31}$$

The expression (30) or (31) for ρ_∞ is a very general result based only on the argument that the static susceptibility reaches a Curie law at high temperatures. So, the resistivity is independent of band-structure effects and of I or the Stoner factor $S = (1 - \bar{I})^{-1}$: again, for infinite T, the paramagnons have vanished and the interaction I between the i electrons must not appear anymore.

Formula (31) is identical to the spin-disorder resistivity of ferromagnetic metals at high temperatures.[33,34] This is a reasonable result: at very high temperatures, the product $I\chi^0(q, \omega, T)$ in formulas (3) becomes negligible compared to 1, since $\chi^0(q, \omega, T)$ is strongly decreased; therefore the i electrons can be regarded as not interacting anymore among themselves and they scatter, then, independently the c electrons as the independently paramagnetic ions in the spin-disorder problem. If we had taken a more realistic I decreasing with increasing temperatures, this would not have changed ρ_∞, but the product $I\chi^0$ would have been even more rapidly reduced, which would yield a more rapid saturation with temperature than in the case of a constant I value. We shall return to the comparison with the spin-disorder problem more extensively in Sec. III D.

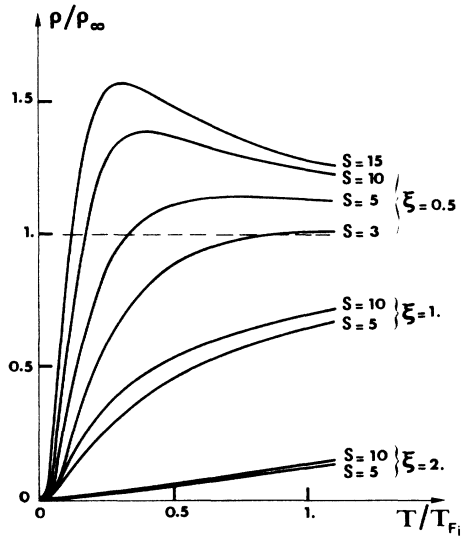

FIG. 6. Computed variation of ρ/ρ_∞ vs T/T_{Fi} for different values of S and $\xi = (k_{Fc}/k_{Fi})$.

B. Resistivity curves

In order to obtain the whole resistivity curves, the expression (1) can be written again as a function of dimensionless parameters:

$$\frac{\rho}{\rho_\infty} = \frac{3}{4\pi} \frac{1}{\bar{T}} \int_0^{2\xi} \frac{\bar{q}^3 d\bar{q}}{\xi^4} \int_0^\infty \mathrm{Im}\bar{\chi}(\bar{q}, \bar{\omega}, \bar{T}) \times \frac{\bar{\omega} d\bar{\omega}}{(e^{\bar{\omega}/\bar{T}} - 1)(1 - e^{-\bar{\omega}/\bar{T}})} , \tag{32}$$

where

$$\bar{\chi}(\bar{q}, \bar{\omega}, \bar{T}) = \frac{\chi(\bar{q}, \bar{\omega}, \bar{T})}{\chi^0(0, 0, 0)} , \quad \bar{q} = \frac{q}{k_{Fi}} , \quad \bar{\omega} = \frac{\omega}{T_{Fi}} , \quad \bar{T} = \frac{T}{T_{Fi}} , \tag{33}$$

and also

$$\xi = k_{Fc}/k_{Fi} . \tag{34}$$

The full temperature dependence of ρ has been obtained by performing a numerical computation on IBM 370. We obtain ρ/ρ_∞ vs T/T_{Fi} with two parameters: ξ, which fixes the relative importance of the q integral appearing in (32), and S, which gives the intensity and the position of the peak in $\mathrm{Im}\chi(q, \omega, T)$.

Figure 6 shows typical plots of ρ for different values of S and ξ. All the resistivity curves start like T^2 at low temperatures and exhibit first a positive curvature, but at more-or-less higher temperature the curvature becomes negative. All the resistivity curves reach ρ_∞ at high temperatures, but the way they reach the saturation ρ_∞ may be different: for ξ of the order of 1 or more, the resistivity increases monotonically from 0 to ρ_∞; for smaller-ξ values, the resistivity curves exhibit a maximum which is more pronounced for increasing S or decreasing ξ.

The influence of S on the resistivity curves can be easily understood, because the intensity of S fixes the importance of the spin fluctuations. We can also understand the effect of ξ as follows: As shown on Fig. 5, the intensity of the peak of $\mathrm{Im}\chi(q, \omega, T)$ decreases with increasing q; so, since the q integral of (32) appears as an average giving a larger weight for larger q, the mean value of the resistivity is smaller for a larger ξ value. Physically, one can compare the role of ξ with the wavelength effect arising in the de Gennes and

Friedel[34] spin-disorder problem. This point will be discussed in more details in Sec. III D.

C. High temperature behavior: Existence of a maximum

If the resistivity saturation is independent of S, the way ρ reaches this limit is, on the contrary, strongly dependent on S and ξ, as shown in Fig. 6. For $T \to \infty$, we can expand the exponentials of (1) in power of ω/T and write

$$\rho \simeq \rho_0 \int_0^{2k_{Fc}} \frac{q^3 dq}{k_{Fc}^4} \left(T \int_0^\infty \frac{2\mathrm{Im}\chi(q,\omega,T)}{\omega} d\omega - \frac{1}{12T} \int_0^\infty 2\omega \mathrm{Im}\chi(q,\omega,T) d\omega \right) . \quad (35)$$

The first term can be transformed into $\chi(q,0,T)$ using (28) and (29), but if we would like to have the corrective term to ρ_∞, we have to expand $\chi^0(q,0,T)$ in $\chi(q,0,T)$ up to the second term in $1/T^2$, i.e.

$$\chi^0(q,0,T) \simeq \frac{n_i}{2\nu} \frac{1}{T} \left(1 - \frac{q^2}{12T} \right) . \quad (36)$$

The following term appearing in (36) comes from the first correction to the Boltzmann distribution and is in $T^{-5/2}$. The first term of (35) can be written as

$$T \int_0^\infty \frac{2\mathrm{Im}\chi(q,\omega,T)}{\omega} d\omega \simeq \frac{\pi}{2} \frac{n_i}{\nu} \left[1 + \left(\bar{I} \frac{k_{Fi}^2}{3} - \frac{q^2}{12} \right) \frac{1}{T} \right] . \quad (37)$$

The second term of (35), which is of order T^{-1}, can be computed by taking for $\mathrm{Im}\chi(q,\omega,T)$ the asymptotic form of $\mathrm{Im}\chi^0(q,\omega,T)$ given by (25), or more simply by the f-sum rule[32]:

$$\int_0^\infty 2\omega\, \mathrm{Im}\chi(q,\omega,T) d\omega \simeq \int_0^\infty 2\omega\, \mathrm{Im}\chi^0(q,\omega,T) d\omega \simeq \frac{\pi n_i}{2\nu} q^2 . \quad (38)$$

So, after performing the integration over q, the resistivity is given, up to the first order in T^{-1}, by

$$\rho \simeq \rho_\infty [1 + \tfrac{2}{3}(\bar{I} - \tfrac{4}{3}\xi^2) T_{Fi}/T] . \quad (39)$$

[Note that there was a misprint in Ref. 11, formula (6), which is obviously identical to our Eq. (39).]

It results that a criterion for the existence of a maximum in the resistivity curve is

$$\bar{I} > \tfrac{4}{3}\xi^2 . \quad (40)$$

This criterion is verified by the results of Fig. 6; in particular, since we always have $\bar{I} < 1$, there is no maximum, regardless of S; for ξ larger than $\frac{1}{2}\sqrt{3}$, as it can be shown in Fig. 6 for the two cases $\xi = 1$ and $\xi = 2$.

The corrective T^{-1} term appearing in (39) depends on all the approximations of the model. Certainly it would be different for realistic band shapes (not parabolic), for a temperature dependent I interaction and with including paramagnon corrections.

But, since a similar T^{-1} correction from the asymptotic ρ_∞ limit appears here as in the de Gennes and Friedel spin-disorder resistivity,[34] we want to show now the details of the comparison between our Eqs. (39) and (31) with the spin-disorder resistivity of de Gennes and Friedel.[34]

D. Comparison with spin-disorder resistivity

The high-temperature spin-disorder resistivity is given by the formulas (3.6), (3.8) and (3.4) of the de Gennes and Friedel paper[34]:

$$\rho_{\infty\, dGF} = \frac{m}{e^2 \xi_{dGF}} \frac{\hbar k_0}{m} \frac{1}{4\pi} \left(\frac{mG}{\hbar^2} \right)^2 S(S+1) . \quad (41)$$

G is the s-f coupling per atom identical to J/ν in our case, k_0 is the Fermi momentum of the conduction electrons identical to our k_{Fc}, ξ_{dGF} is the number of conduction electrons per magnetic ion, so that, in our notations, when each f electron of spin $\frac{1}{2}$ replaces each magnetic ion of spin S, one has the identification

$$G \equiv J/\nu, \quad k_0 \equiv k_{Fc}, \quad \xi_{dGF} \equiv n_c/n_i, \quad S = \tfrac{1}{2} . \quad (42)$$

Then one writes in our notations

$$\rho_{\infty\, dGF} = \frac{3}{16\pi} \frac{n_i}{n_c} \frac{m_c^3 J^2}{e^2 \hbar^3 \nu^2} k_{Fc} . \quad (43)$$

Then using $\hbar/\tau_{Fc} = \hbar^2 k_{Fc}^2 / 2m_c$ and $N(\epsilon_{Fc}) = m_c k_{Fc}/\pi^2 \hbar^2 \nu$, we have

$$\rho_{\infty\, dGF} = \frac{\pi}{8} [JN(\epsilon_{Fc})]^2 \frac{m_c}{n_c e^2 \tau_{Fc}} \frac{n_i}{n_c} , \quad (44)$$

which is identically our formula (31).

Now, the critical temperature of de Gennes and Friedel[34] is given by their formula (5.3):

$$T_{c\, dGF} = \tfrac{2}{3} J_{dGF} v S(S+1) \quad (45)$$

v is the number of nearest neighbors of a given ion; J_{dGF} is the interaction between two ions and has to be identified with the interaction I between the i electrons here. Identifying v with n_i/ν, we get

$$T_{c\, dGF} = \tfrac{1}{2} I n_i/\nu , \quad (46)$$

which may be rewritten as

$$T_{c\, dGF} = \tfrac{2}{3} \bar{I} T_{Fi} . \quad (47)$$

Furthermore the formula (5.8) of de Gennes and Friedel can be written at high temperature:

$$\left(\frac{\rho}{\rho_\infty} \right)_{dGF} = \frac{1}{4} \int_0^2 x^3 dx \left(1 + \frac{T_c}{T} \frac{\sin(k_0 dx)}{k_0 dx} \right) . \quad (48)$$

If one supposes the distance d between the scatterers (the i-electrons in our case) to be very small, the above formula can be expanded in powers of $k_0 d$:

$$\left(\frac{\rho}{\rho_\infty}\right)_{dGF} \simeq 1 + \frac{T_{c\,dGF}}{T}\left[1 - \tfrac{4}{9}(k_{Fc}d)^2\right] \qquad (49)$$

This formula has to be compared with our formula (39), which can be rewritten as

$$\frac{\rho}{\rho_\infty} \simeq 1 + \frac{2\bar{I}T_{Fi}}{3T}\left[1 - \frac{4}{3\bar{I}}\left(\frac{k_{Fc}}{k_{Fi}}\right)^2\right] . \qquad (50)$$

The comparison of (49) and (50) is particularly striking: we just identified, above, $\rho_{\infty\,dGF}$ with our ρ_∞ and $T_{c\,dGF}$ with our $\frac{2}{3}\bar{I}T_{Fi}$; moreover in the remaining brackets, we have the same wavelength effect as de Gennes and Friedel. If we suppose the distance between the scatterers to be much smaller than the conduction-electron wavelength, their formula is similar to ours if one assimilates d^2 with $3/\bar{I}k_{Fi}^2 = (2/I)(v/n_i)$. This is reasonable: the phenomenological interaction I in the paramagnon model is very short range; actually it is taken to be a contact interaction, so that the identification between d^2 and $(2/I)(v/n_i)$ is not strict although physical.

However, one can discuss the role of our parameter ξ in the same way as the role of the parameter $k_0 d$ of de Gennes and Friedel; when this parameter increases, the wavelength of the interacting electrons becomes larger than the conduction-electron wavelength and thus the intensity of the scattering decreases leading to a smaller resistivity for larger ξ, as it has been shown on the numerical results.

In their discussion of the wavelength effect, de Gennes and Friedel noticed that for large $k_{Fc}d$ the correlation effect is small, while for small values of that parameter one expects a large correlation effect and an important increase of the resistivity in the neighborhood of T_c, in which case the molecular-field approximation has to be refined. This is quite true in our case, too. The RPA approximation should be improved at lower temperature by including higher-order paramagnon corrections, as was already indicated in Sec. II A.

We wish also to point out here the following remark: $T_{c\,dGF}$ in the de Gennes-Friedel case is the critical temperature separating the disordered paramagnetic region from the ordered ferromagnetic one. Here we never reach a magnetic ordering, since the system remains paramagnetic over the whole temperature range; however, the temperature $\frac{2}{3}\bar{I}T_{Fi} = T_{c\,dGF}$ corresponds to a smooth transition between a high-temperature region, where the i electrons act almost independently (cf. the disordered region of de Gennes and Friedel), and a low-temperature region, where the i electrons act as strongly interacting ones under the form of paramagnons (cf. the ordered region of de Gennes and Friedel). From that point of view, the larger is $\bar{I}$ and thus the wider is the temperature range $0 \le T \le T_{c\,dGF} = \frac{2}{3}\bar{I}T_{Fi}$ where the paramagnons are important. Moreover, when S is stronger, the spin-fluctuation temperature is smaller and so is the temperature of the maximum. This effect of S is shown numerically in Table I, where we have reported, for different S and ξ values, $T_{c\,dGF} = \frac{2}{3}\bar{I}T_{Fi}$, the spin-fluctuation temperature $T_{sf} = T_{Fi}/S$ and the numerically computed temperature T_m and value ρ_m of the resistivity maximum.

E. Low-temperature behavior: Comparison with previous theories

1. *Low-temperature behavior*

The T^2 term at low temperature is directly obtained by use of the expansion of $\mathrm{Im}\chi(q,\omega,T)$ up to the first order in ω and T. So, for $\mathrm{Re}\bar{\chi}^0(q,\omega,T)$ we use the expression (20) giving $\bar{\chi}^0(q,0,0)$ and for $\mathrm{Im}\bar{\chi}^0(q,\omega,T)$ we use:

$$\mathrm{Im}\bar{\chi}^0(q,\omega,T) = \frac{\pi}{2}\frac{\omega}{v_{Fi}q} = \frac{\pi}{4}\frac{\bar{\omega}}{\bar{q}} \quad \text{for } q < 2k_{Fi}$$

$$= 0 \qquad \text{otherwise} \qquad (51)$$

Since the expressions (20) and (51) are also a first-order expansion in ω and T for $\bar{\chi}^0(q,\omega,0)$, the low-temperature T^2 term is exactly the same here, in our case of a temperature-dependent susceptibility, than in the previous case where one has taken $\chi(q,\omega,0)$ in the whole temperature range.

This T^2 term is given by

$$\frac{\rho}{\rho_\infty} \simeq A\left(\frac{T}{T_{Fi}}\right)^2 , \qquad (52)$$

with

$$A = \frac{\pi^2}{16}\int_0^{2\min\{\xi,1\}} |S(q)|^2 \frac{\bar{q}^2 d\bar{q}}{\xi^4} \qquad (53)$$

and

$$S(q) = [1 - \bar{I}\bar{\chi}^0(q,0,0)]^{-1} . \qquad (54)$$

After this T^2 term, the resistivity increases, but there is a change of curvature at a more-or-less high temperature; so one cannot speak strictly of a linear behavior, perhaps only in the region where the change of curvature occurs. The previous linear behavior was obtained as an asymptotic high-temperature behavior in the case of a temperature-independent susceptibility. In order to compare with the exact behavior, let us derive this T term. It can be obtained just by replacing $\chi^0(q,0,T)$ in (29) by $\chi^0(q,0,0)$, so that it is given by

$$\rho/\rho_\infty \simeq B(T/T_{Fi}) , \qquad (55)$$

where

$$B=\frac{3}{8}\int_0^{2\xi}\chi^0(q,0,0)S(\bar{q})\frac{\bar{q}^3 d\bar{q}}{\xi^4}\,. \tag{56}$$

The comparison between the two cases of temperature-dependent and temperature-independent susceptibility is shown in Fig. 7. In Fig. 7 we have plotted the resistivity curves computed directly by the general formula (1) by use of $\chi(q,\omega,T)$ [curves (1)] or by use of $\chi(q,\omega,0)$ instead of $\chi(q,\omega,T)$ [curves (2)] for $S=10$ and for two values of ξ: $\xi=0.5$ and $\xi=1$. In this figure one can observe the importance of the departure from the T law arising in the region of $T_{sf}=T_{Fi}/S$.

But let us now compare the behaviors with previous theories which correspond generally to an approximation for the curves (2) of Fig. 7.

2. *Comparison with previous theories*

Approximate analytical expressions can be obtained to describe the T^2-T behavior in the case of temperature-independent susceptibility.

If we approximate $\chi^0(q,\omega,T)$ in the whole frequency range by its low-frequency first-order expansion given by (20) and (51), we obtain

$$\mathrm{Im}\chi(q,\omega,0)=S(q)\frac{\tilde{\omega}_q}{1+\tilde{\omega}_q^2}\,, \tag{57}$$

where $\tilde{\omega}_q$ is a q-dependent reduced frequency given by

$$\tilde{\omega}_q=\frac{\pi}{2}\frac{\omega}{v_{Fi}q}S(q)=\frac{\pi}{4}\frac{\bar{\omega}}{\bar{q}}S(q)\,. \tag{58}$$

In (58), we assume $\bar{I}$ close to 1.

So, within this approximation for χ^0, we obtain a Lorentzian shape for $\mathrm{Im}\chi$ which is maximum for $\tilde{\omega}_q=1$; i.e., for $\omega=(2/\pi)v_{Fi}q/S(q)$. The discrepancies with the exact shape given by Fig. 5 for $T=0$ are (i) a small shift of the maximum due to the neglect of the ω dependence of $\mathrm{Re}\chi^0(q,\omega,0)$, and (ii) the introduction of tails for large ω values where (20) and (51) are no longer valid.

Then the resistivity takes the form

$$\frac{\rho}{\rho_\infty}=\frac{3}{\pi^2}\int_0^{2\min\{\xi,1\}}\frac{\bar{q}^4 d\bar{q}}{\xi^4}\frac{1}{\tilde{T}_q}\times\int_0^\infty\frac{\tilde{\omega}_q^2 d\tilde{\omega}_q}{(e^{\tilde{\omega}_q/\tilde{T}_q}-1)(1-e^{-\tilde{\omega}_q/\tilde{T}_q})(1+\tilde{\omega}_q^2)}\,, \tag{59}$$

with

$$\tilde{T}_q=\frac{\pi}{2}\frac{T}{v_{Fi}q}S(q)=\frac{\pi}{4}\frac{\bar{T}}{\bar{q}}S(q)\,. \tag{60}$$

Then, we recognize the T^2-T function of Kaiser and Doniach[2]:

$$f(\tilde{T})=\frac{1}{\tilde{T}}\int_0^\infty\frac{\tilde{\omega}^2 d\tilde{\omega}}{(e^{\tilde{\omega}/\tilde{T}}-1)(1-e^{-\tilde{\omega}/\tilde{T}})(1+\tilde{\omega}^2)}\,. \tag{61}$$

In the case of alloys, this function describes directly the spin-fluctuation resistivity curve, but here one has to integrate over q, and the resistivity is given by

$$\frac{\rho}{\rho_\infty}=\frac{3}{\pi^2}\int_0^{2\min\{\xi,1\}}f\left(\frac{\pi}{4}\frac{\bar{T}}{\bar{q}}S(\bar{q})\right)\frac{\bar{q}^4 d\bar{q}}{\xi^4}\,. \tag{62}$$

Using the change of variable $z=1/2\pi\tilde{T}$, the function $f(\tilde{T})$ can be expressed in term of the digamma function $\psi(z)$[35]:

$$f\left(\frac{1}{2\pi z}\right)=-\frac{1}{2}-\frac{1}{4z}+\frac{z}{2}\frac{\partial\psi(z)}{\partial z}\,. \tag{63}$$

So, using the following expansions[35]:

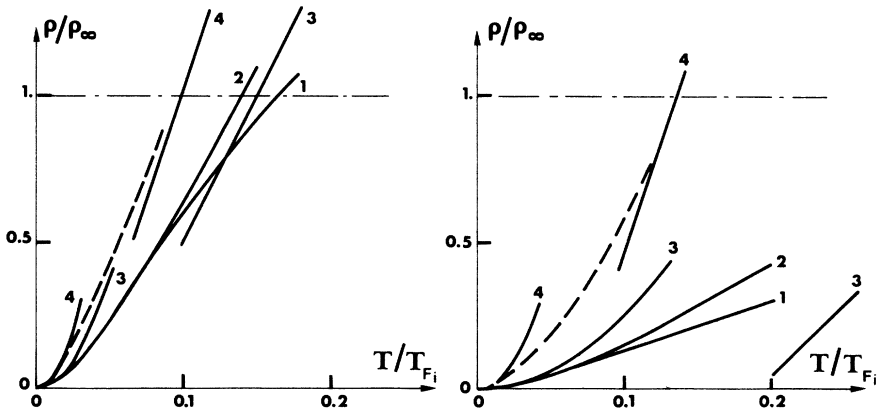

FIG. 7. Low-temperature part of the resistivity curves for $S=10$ and two values of ξ: $\xi=0.5$ (left-hand part of the figure) and $\xi=1$ (right-hand part of the figure), as explained in text: the curves labeled (1) and (2) correspond, respectively, to the exact computed resistivities with temperature dependent and temperature independent Stoner susceptibility. The parabolas and straight lines, (3) and (4), correspond to approximate analytical derivations of the low- and high-temperature limits, respectively, with [approximation (a)] or without [approximation (b)] taking into account the $q^2/12$ term in $S(q)$.

$$\frac{\partial\psi(z)}{\partial z} \simeq \frac{1}{z} + \frac{1}{2z^2} + \frac{1}{6z^3} + \cdots \quad \text{when } z \to \infty ,$$
$$\frac{\partial\psi(z)}{\partial z} = \frac{1}{z^2} + \frac{\pi^2}{6} \quad \text{when } z \to 0 , \tag{64}$$

the asymptotic forms of $f(\bar{T})$ are $\frac{1}{3}\pi^2\bar{T}^2$ at low temperature and $\frac{1}{2}\pi\bar{T} - \frac{1}{2}$ at high temperatures. Thus, formula (62) is characteristic of a curve starting as T^2 at low temperatures and reaching an asymptotic linear T law at high temperatures. These asymptotic behaviors are given by

For $T \to 0$,

$$\frac{\rho}{\rho_\infty} \simeq A\left(\frac{T}{T_{Fi}}\right)^2 , \tag{65}$$

with

$$A = \frac{\pi^2}{16}\int_0^{2\min\{\xi,1\}} |S(\bar{q})|^2 \frac{\bar{q}^2 d\bar{q}}{\xi^4} . \tag{66}$$

We recognize the same T^2 term as in the exact case [formulas (52) and (53)].

For $T \to \infty$,

$$\frac{\rho}{\rho_\infty} \simeq B\left(\frac{T}{T_{Fi}}\right) - \frac{48}{5\pi^2}\frac{(\min\{\xi,1\})^5}{\xi^4} , \tag{67}$$

with

$$B = \frac{3}{8}\int_0^{2\min\{\xi,1\}} S(\bar{q})\frac{\bar{q}^3 d\bar{q}}{\xi^4} . \tag{68}$$

Equation (68) appears as an approximation of (56) by taking an Heaviside function for $\chi^0(q,0,0)$ with a cutoff at the Kohn anomaly instead of the exact q-dependent curve.

At this step, the analytical expressions of A and B will depend on the approximate analytical expression used for $S(\bar{q})$.

Approximation (a). The small-q expansion of $\chi^0(q,0,0)$ usually taken in the low temperature theories leads to

$$S(q) \simeq \frac{1}{1 - \bar{I} + \frac{1}{12}\bar{I}q^2} . \tag{69}$$

Assuming $\xi < 1$, we find the following analytical expressions for A and B:

$$A_a = \frac{9\pi^2}{4\xi^4}(\tfrac{1}{3}S)^{1/2}\left(\arctan[\xi(\tfrac{1}{3}S)^{1/2}] - \frac{\xi(3S)^{1/2}}{3+\xi^2 S}\right) , \tag{70}$$

$$B_a = \frac{9}{\xi^2}\left(1 - \frac{3}{\xi^2 S}\ln(1+\tfrac{1}{3}\xi^2 S)\right) . \tag{71}$$

Expression (70) was already given by Mills.[36]

Approximation (b). For very-small-ξ values, if $\frac{1}{12}\bar{I}\bar{q}^2_{\max}$ $(=\frac{1}{3}\bar{I}\xi^2)$ is much smaller than $1-\bar{I}$, i.e., $\xi^2 \ll 3(1-\bar{I})/\bar{I}$, one can then drop the q^2 term in the denominator of (69) and one gets

$$S(q) \simeq \frac{1}{1-\bar{I}} = S . \tag{72}$$

This approximation is the one considered by Mills and Lederer[1] in their first derivation of the low-temperature T^2 term.

The corresponding values of A and B are the asymptotic forms of A_a and B_a when $\xi \to 0$ and are given by

$$A_b = \frac{\pi^2}{6}\frac{S^2}{\xi} , \tag{73}$$

$$B_b = \tfrac{3}{2}S . \tag{74}$$

In order to compare the approximations (a) and (b) with the exact curves (1) and (2) of Fig. 7, we have reported, in the same figure, the two parabolas corresponding to (65) [with (70) and (73)] and the two straight lines corresponding to (67) [with (71) and (74)]. So, the curves labeled (3) and (4) in Fig. 7 correspond, respectively, to the approximations (a) and (b).

Then, we can finally make some remarks.

(i) In Fig. 7, we see clearly that the approximation (a) and (b) are very rough for large ξ, as $\xi = 1$. When ξ is smaller they become realistic and obviously the approximation (a) is always better than the approximation (b).

(ii) For very small ξ values, when approximation (b) is valid, one notes a scaling in T^2/T_{sf}^2 and T/T_{sf} for the low-temperature behavior of ρ. Kaiser and Doniach[2] found a similar scaling in the case of alloys, but Mills[36] pointed out that this scaling does not hold in general; indeed; as we see here, it depends very much of the value of the enhancement (as shown by Mills[36]) but also of the value of ξ.

(iii) These analytical results permit a better description of the respective roles of S and ξ. When ξ tends to zero, the opposite roles of S and ξ appear clearly, since formula (73) involves only S^2/ξ. In this very small ξ limit, the resistivity behaves at low temperatures as

$$\frac{\rho}{\rho_\infty} \sim \frac{\pi^2}{6}\frac{S^2}{\xi}\left(\frac{T}{T_{Fi}}\right)^2 = \frac{\pi^2}{6}\left(\frac{T}{T_{sf}\sqrt{\xi}}\right)^2 . \tag{75}$$

(iv) Since there exists a scaling in $(T/T_{sf}\sqrt{\xi})^2$ for very small ξ at low temperature, it looks interesting to compare the temperature T_m of the resistivity maximum to $T_{sf}\sqrt{\xi}$. Table II gives $T_m/T_{sf}\sqrt{\xi}$ for the values of S and ξ of Table I. According to Table II, this ratio is reasonably constant and we estimate T_m to be roughly given by

$$T_m \simeq 5T_{sf}\sqrt{\xi} = 5T_{Fi}(\sqrt{\xi})/S . \tag{76}$$

This formula can be very useful for analyzing the experimental data.

(v) According to Table I, the larger the S and the smaller the ξ, the smaller the T_m and the larger the ρ_m: this is in perfect agreement with the anal-

TABLE I. Values of the critical temperature of de Gennes-Friedel $T_{c\,dGF}/T_{Fi}$, of the spin-fluctuation temperature T_{sf}/T_{Fi}, of the temperature T_m/T_{Fi} and the resistivity ρ_m/ρ_∞ at the maximum of the resistivity curves, for different S and ξ values.

S		3	5	10
$T_{c\,dGF}/T_{Fi}$		0.44	0.53	0.60
T_{sf}/T_{Fi}		0.33	0.20	0.10
T_m/T_{Fi}	$\xi=0.2$	0.78	0.47	0.25
	$\xi=0.3$	0.94	0.57	0.29
	$\xi=0.5$	>1	0.73	0.38
ρ_m/ρ_∞	$\xi=0.2$	1.26	1.53	2.11
	$\xi=0.3$	1.16	1.38	1.85
	$\xi=0.5$	•••	1.13	1.38

ysis in Sec. III D on the high-temperature results where we noted that the effects of the correlations are larger for smaller ξ and larger S. We remark also that, according to Table II, the product $(\rho_m/\rho_\infty)(T_m/T_{Fi})^{1/2}$ is practically constant and close to 1:

$$\rho_m/\rho_\infty \sim (T_{Fi}/T_m)^{1/2} \quad . \tag{77}$$

IV. COMPARISON WITH EXPERIMENTS

A. Experimental situation

The improvement brought by the present theory with respect to the previously obtained T^2 and T laws for the spin-fluctuation resistivity concerns the clear departure of the high-temperatures resistivity from the T law, with the possible occurrence of a maximum. We would like to review here the experimental situation of spin-fluctuation systems, with special attention paid to the high-temperature domain.

Our present study of extended spin fluctuations can be applied as it stands only to pure metals and compounds. Extension to local paramagnons involving $\sum_{\vec{q}} \chi^0(q,\omega,T)$ would be needed to account for dilute alloys with nearly magnetic impurities and is not included in this paper. The resistivity of some semimetals like V_2O_3[29] or ytterbium[28] close to the metal-semiconductor transition also exhibits a tendency to saturation at high T which would certainly involve, as in our case, the temperature dependence of the correlation function; but, to start with, the model is different, and our calculation cannot be simply extended to include those cases.

TABLE II. Values of the rations $T_m/T_{sf}\sqrt{\xi}$ and $(\rho_m/\rho_\infty)(T_m/T_{Fi})^{1/2}$ for the S and ξ values reported in Table I.

S		3	5	10
$\frac{T_m}{(T_{sf}\sqrt{\xi})}$	$\xi=0.2$	5.2	5.2	5.6
	$\xi=0.3$	5.2	5.2	5.3
	$\xi=0.5$	•••	5.2	5.4
$\frac{\rho_m}{\rho_\infty}\left(\frac{T_m}{T_{Fi}}\right)^{1/2}$	$\xi=0.2$	1.11	1.05	1.05
	$\xi=0.3$	1.12	1.04	1.00
	$\xi=0.5$	•••	0.97	0.85

In the transition elements series, palladium[12] and platinium[13] are the two well-known exchange-enhanced paramagnetic metals. The resistivity of palladium presents a small T^2 term at low temperatures with a coefficient $A_{exp}=\rho/T^2$ equal to 3×10^{-5} $\mu\Omega$ cm/K^2,[1] and then increases linearly with temperature as shown on Fig. 8. Moreover, both resistivities of platinum and palladium depart from a linear law at high temperatures. If we call T_d the temperature at which the resistivity departs from the T law, T_d is roughly equal to 300 or 400 K, respectively, in the palladium and the platinum.

In the rare-earth series, only α-cerium is known to be an exchange-enhanced paramagnetic metal[37] with a large Stoner enhancement factor.[17,37] The resistivity of α-cerium at normal and high pressure has been recently measured by several authors, but the present results are controversial. Katzman and Mydosh[15] have found, at low temperature, a large T^2 term which is rapidly decreasing with pressure; on the contrary, Brodsky and Friddle,[16] Grimberg *et al.*,[17] and Nicolas-Francillon and Jerome[14] have found either no T^2 term or a very small one in a pure α-cerium sample which contains no β-phase. Then the resistivity of α-cerium increases linearly with temperature, but there also exists a controversy as to whether there

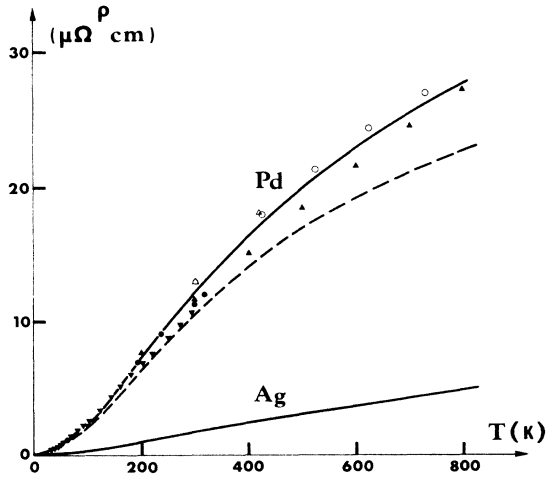

FIG. 8. Fit of the resistivity of Palladium; (▼, ▲, ●, ○, △) experimental data of Pd (Ref. 12): ▼ according to White and Woods, ▲ according to Ricker and Pflüger, ● and ○ according to Schindler *et al.*, △ according to Epelboin and Vapaille; (- - - - -) the theoretical resistivity with $S=10$, $\xi=1$, $\rho_\infty=47$ $\mu\Omega$ cm, $T_{Fi}=2000$ K; (——) the total theoretical resistivity obtained by adding the resistivity of Ag (Ref. 44).

is a negative curvature at high temperatures. Katzman and Mydosh[15] and Nicolas-Francillon and Jerome[14] have found a slight departure from the T law at 60–80 K, but Brodsky and Friddle[16] have obtained a linear law up to the highest measured temperature. Thus, the experimental situation of α-cerium is not sufficiently clear to allow a direct comparison with our study.

The most conclusive cases concern the resistivities of actinide metals and compounds. The resistivity of neptunium has an important T^2 term with a coefficient $A_{exp} = 2\times10^{-3}$ $\mu\Omega$ cm/K^2,[3] begins to depart from the T law at $T_d = 80$ K, and saturates between 300 and 500 K, as shown on Fig. 9.[18] The resistivity of plutonium behaves as T^2 at low temperatures with A_{exp} of order 10^{-2} $\mu\Omega$ cm/K^2 ($A_{exp} = 0.021$ $\mu\Omega$ cm/K^2 for single-crystal monoclinic α-Pu with the current along the [010] direction[3]), then departs from the linear law at $T_d = 40$ K and reaches a maximum of order 160 $\mu\Omega$ cm at roughly 100 K, as shown in Fig. 10.[18–22] The maximum is more pronounced with a lower maximum temperature for the single-crystal Pu with the current along the [010] direction, while the resistivity remains almost constant from 120 to 300 K for the single-crystal Pu with the current along the [100] direction, as also shown in Fig. 10.[19] However, the magnetic susceptibilities of both neptunium[38] and plutonium[38,39] remain roughly constant up to 300 K.

The maximum of the resistivity curve becomes less pronounced when small amounts of aluminum,[24] cerium,[24] scandium,[25] or neptunium[23] are diluted in plutonium. The same type of resistivity curve with a maximum exists in Pu_6Fe,[40] Pu_3Al,[40] or $PuAl_2$[3] compounds. In particular, the resistivity

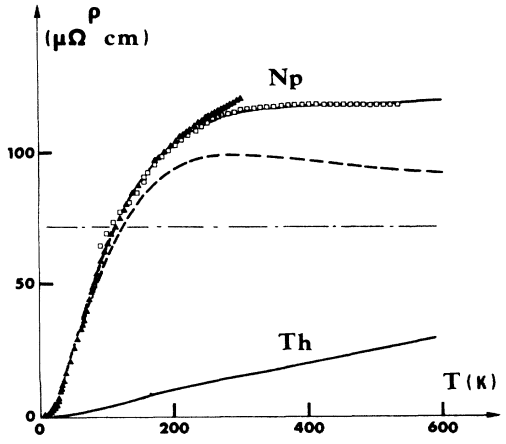

FIG. 9. Fit of the resistivity of Np; (▲,■) experimental data of Np according to Meaden (Ref. 18); (- - - - -) the theoretical resistivity with $S=10$, $\xi=0.5$, $\rho_\infty=71.5$ $\mu\Omega$ cm, $T_{Fi}=750$ K; (——) the total theoretical resistivity obtained by adding the resistivity of Th (Ref. 22).

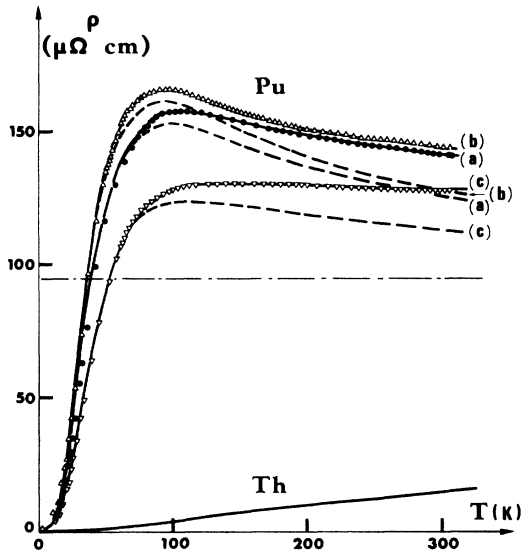

FIG. 10. Fits of the resistivities of a randomly oriented (a) sample of Pu and of monocrystals with the (010) direction parallel (b) and perpendicular (c) to the current; (●), (△), and (▽) experimental data (Ref. 23) corresponding, respectively, to the cases (a), (b), (c); (- - - -) the theoretical resistivities with $S=10$, $\rho_\infty=95$ $\mu\Omega$ cm, $T_{Fi}=280$ K and different ξ values: $\xi=0.4$, 0.37, 0.53, respectively, for the cases (a), (b), (c); (——) the total theoretical resistivities obtained by adding the resistivity of Th (Ref. 22).

of $PuAl_2$ is quite surprising, with an enormous A_{exp} coefficient equal to 0.94 $\mu\Omega$ cm/K^2 for the T^2 law, a maximum of order 220 $\mu\Omega$ cm at a temperature smaller than 10 K and a rapid decrease to reach at room temperature the same resistivity as that of plutonium itself. The $PuAl_2$ magnetic susceptibility has a Curie-Weiss temperature dependence at high temperatures and deviates from this at low temperatures, but there is no evidence of localized magnetic moment.[3]

Other compounds present a resistivity that saturates at high temperature, like that of neptunium. This is, for example, the case of UAl_2,[3] $PuRh_2$,[41] $PuIr_2$,[41] $PuRu_2$,[41] and $NpRh_3$.[42,43] On one side, the resistivities of UAl_2,[3] $PuRh_2$,[41] and $NpRh_3$[43] behave as T^2 at low temperatures with A_{exp} coefficients respectively equal to 0.27, 0.127, and 5×10^{-3} $\mu\Omega$ cm/K^2 and T_d temperatures respectively equal to 20, 30, and 90 K. Furthermore the magnetic susceptibilities of these three compounds decrease appreciably with temperature. On the other side, no T^2 term was found in the resistivity of $PuIr_2$ and $PuRu_2$[41] at low temperatures, the T_d temperatures are relatively large (of order 75 K) and their magnetic susceptibilities are roughly constant up to room temperature, as in the case of Np and Pu.

TABLE III. Values of the A_{exp} coefficient for the low-temperature T^2 law and of the temperature T_d at which the resistivity departs from the T law for different metals and compounds.

	A_{exp} ($\mu\Omega$ cm/K^2)	T_d (K)
Pt		400
Pd	3×10^{-5}	300
Np	2×10^{-3}	80
$NpRh_3$	5×10^{-3}	90
$PuIr_2$		75
$PuRu_2$		75
Pu	10^{-2} {0.021 for (010) Pu}	40
$PuRh_2$	0.127	30
UAl_2	0.27	20
$PuAl_2$	0.94	5

B. Analysis of the experimental data

Table III gives the values of A_{exp} and T_d for all the metals and compounds reviewed in the last paragraph. The existence of spin fluctuations is apparently established for all the systems of Table III.[3,41-43] Two reasons support this hypothesis: first, these materials have a large T^2 term in the low-temperature resistivity; then according to Arko *et al.*,[3] the ratio of the total densities of states deduced from magnetic susceptibility and electronic specific-heat constant is, respectively, 2.9 for α-Np and 2.1 for α-Pu. But if we remember that these metals have 7*s*, 6*d*, and 5*f* bands and that essentially the magnetic susceptibility of the 5*f* electrons is exchange enhanced, and moreover if we take into account the mass enhancement effect for the electronic specific-heat constant, we find Stoner enhancement factors of order 10 for both Np and Pu.

So, we apply the preceding theoretical model to the systems listed in Table III. The interacting band i is the d band for Pd and Pt, while it is the f band for rare earths and actinides. In the case of Np and Pu metal and compounds, we consider that the i band is the very narrow 5*f* band and the c band is formed by the 7*s* and 6*d* bands and we neglect here the d-f hybridization. We will come back to this point later on.

First, two interesting comments can be drawn from Table III: (a) There is a connection between A_{exp} and T_d; the value of T_d decreases when the A_{exp} coefficient increases or when the material is closer to becoming magnetic. This result agrees with the model for which the saturation at high temperatures is clearly linked to the importance of the paramagnons yielding the T^2 law. (b) The temperature T_d is larger by an order of magnitude for Pd and Pt than for the actinides, while the A_{exp} coefficient of Pd is smaller by at least two orders of magnitude than the A_{exp} coefficients of actinides. Since the Fermi energy T_{Fi} is larger by an order of magnitude for d bands than for f bands, this result agrees with the theory where T_d varies as T_{Fi} and A_{exp} as $1/(T_{Fi})^2$. It results also that the resistivity is smaller for d metals than for f metals.

Then, we can present the fits of the resistivities for palladium, neptunium, and plutonium. These three metals have a large exchange-enhancement factor, chosen here equal to 10. We assume that the resistivity is the sum of the paramagnon resistivity given by the theory and of the phonon resistivity; this small contribution is supposed to be equal to the total resistivity of neighboring normal metals: silver[44] for the fit of Pd, and thorium[22] for the fits of Np and Pu. The value of T_{Fi} is chosen to be some 10^3 K for Pd and some 10^2 K for Np and Pu, which is reasonable, although too small, for d and f bands. At last, the values of ρ_∞ and especially of the unknown ξ parameter are chosen for the best fit of the experimental curves.

Figure 8 shows the experimental resistivities of palladium and silver and also the theoretical resistivity (in full line) obtained by the sum of the phonon resistivity, i.e. that of silver,[44] and of the theoretical paramagnon resistivity (in dashed line) plotted for $S=10$, $T_{Fi}=2000$ K, $\xi=1$, and $\rho_\infty=47$ $\mu\Omega$ cm. But because of the uncertainty in ξ, the theoretical fit of Fig. 8 is certainly not the only one.

Figure 9 shows the experimental resistivities of neptunium and thorium, as well as the theoretical plot for Np. The resistivity of Np is almost constant from 300 to 550 K, so that the paramagnon resistivity has a maximum at roughly 300 K. The parameter ξ is chosen here equal to 0.5, in order to have such a maximum. We have taken here $S=10$, $T_{Fi}=750$ K, $\xi=0.5$, and $\rho_\infty=71.5$ $\mu\Omega$ cm in order to have a very good theoretical fit to the experimental data. These values are slightly different from those reported previously,[11] in order to make a better fit to the high-temperature plateau.

Figure 10 shows the experimental resistivities of Plutonium either (a) with a maximum for a polycrystal, or (b) with a more pronounced maximum for a monocrystal with the current along the (010) axis, or (c) with a plateau from 120 to 300 K for a monocrystal with the current along the [100] axis. In the cases (a) and (b), the total resistivities exhibit a maximum so that the ξ parameter has to be small; in the case (c), ξ is a little larger to give a maximum only for the paramagnon resistivity. So, the theoretical fits have been obtained for: $S=10$, $T_{Fi}=280$ K, $\rho_\infty=95$ $\mu\Omega$ cm, and three different ξ values: $\xi=0.4$ for the case (a), $\xi=0.37$ for the case (b), and $\xi=0.53$ for the case (c). The choice of different ξ values for fitting the highly anisotropic resistivity of α-Pu single crystals can be qualitatively understood because the Fermi sur-

face of plutonium is certainly complicated and anisotropic; however, we cannot compute quantitatively this effect. The ρ_∞ limits have practically the same value for Np and Pu, which is consistent with similar conduction bands and number of $5f$ electrons; but in order to obtain a pronounced maximum for Pu, we must choose different T_{Fi} and ξ values without any clear justification in the parabolic band model.

So, very good fits have been obtained for Pd, Np, and Pu. We have not fitted the data on platinum because it has a small Stoner factor, nor that on α-cerium because they are presently controversial. Acording to Fig. 6, it would be possible to fit the data on $PuAl_2$ by for example taking the same ρ_∞ and T_{Fi} as for Pu, but a much smaller ξ and larger S than in Pu, in order to obtain its extremely pronounced maximum. The curves of $PuIr_2$, $PuRu_2$, $PuRh_2$, UAl_2, and $NpRh_3$ compounds can be fitted by taking a ξ value of order 0.5 to avoid a maximum as in the case of Np; the S values have to be chosen very large for UAl_2 and $PuRh_2$ and smaller for the three other compounds.

At last, the high-temperature decrease of the resistivity of plutonium is less pronounced when pressure is applied up to 13 kbar.[22] Figure 6 indicates that this variation can be described by a decrease of S for increasing pressure, as a result of the weaker f character in actinides as well as in rare earths under pressure.[37] It is worthwhile to note that the change in the density of states amplified by the effect of S in a nearly magnetic metal can be experimentally observed, while the simple change in the density of states in a normal metal would have been too small to be seen: this fact is a strong argument for the present paramagnon model.

However, the value of T_{Fi} used for plutonium is very small—on the order of room temperature—and furthermore, according to Fig. 3 for $q=0$, the temperature variation of the Stoner susceptibility for the i band must be very large to account for the observed behavior of ρ. The magnetic susceptibility of $PuAl_2$ and UAl_2 have a Curie-Weiss temperature dependence at high temperatures and deviate from this at low temperatures; similarly the magnetic susceptibility of $NpRh_3$ and $PuRh_2$ decreases appreciably with temperature. So, these results on the magnetic susceptibility are in good agreement with the theoretical model and consistent with the results on the resistivity.

But, on the contrary, the total observed magnetic susceptibility of Pu, Np, $PuIr_2$, and $PuRu_2$ is almost temperature independent up to room temperature, although the theoretical Stoner susceptibility of the i band has to decrease rapidly with temperature to account for the observed behavior of ρ. So, there are spin-fluctuation systems which present a temperature-independent susceptibility; according to Table III, these systems have smaller A_{exp} values and larger T_d temperatures. The recent study[41] of the four compounds $PuPt_2$, $PuRh_2$, $PuIr_2$, and $PuRu_2$ is very illustrative of this point of view: $PuPt_2$ has a localized magnetism with ferromagnetic ordering below 6 K and the resistivity curve is typical of a magnetic compound. The effect of paramagnons is important in $PuRh_2$, because A_{exp} is large and T_d small, and correspondingly the magnetic susceptibility decreases appreciably with temperature. At last, the two compounds $PuIr_2$ and $PuRu_2$, which have resistivities with larger T_d values, have roughly constant magnetic susceptibilities up to room temperature.

So, for the spin-fluctuation system in actinides, the decrease of the magnetic susceptibility appears generally to indicate larger exchange-enhancement factor than the negative curvature of the high-temperature resistivities: this point is not clearly understood here. But our present model for actinides is greatly oversimplified, because the bands are taken to be parabolic, the $5f$ band is assumed to be extremely narrow, and the d-f hybridization is neglected.[30] Moreover, the total observed susceptibility contains a large $6d$ contribution in addition to the temperature-dependent $5f$ contribution. For all these reasons, the relation between the susceptibility of our i band and the total observed susceptibility is not obvious.

Another explanation[42,45] has been proposed to explain the different behaviors of the magnetic susceptibilities: the spin-fluctuation systems which experimentally exhibit a temperature dependent susceptibility are of the nearly ferromagnetic type, like those studies here, while those which exhibit a temperature-independent susceptibility would be of the nearly antiferromagnetic type.

We think that a better relation between the resistivity and the magnetic susceptibility of nearly magnetic actinides would need a better description of the band shapes, of the d-f hypbridization and also of the paramagnon corrections to χ^0. We wish to note, too, that these effects (not included here) and especially the combination of them may act differently on static properties (susceptibility) and dynamic properties (resistivity), so that it is difficult at this point to relate quantitatively the temperature dependence of the measured total susceptibility and the temperature variation of the susceptibility of our i band used to account for the observed resistivity.

C. Concluding remarks

Taking into account the explicit temperature dependence of the Stoner susceptibility gives a high-temperature saturation for the paramagnon resistivity and a possible maximum at lower tempera-

tures. The theoretical model has been applied successfully to the resistivities of palladium, neptunium, plutonium, and plutonium compounds. However, we cannot really connect in our simplified model the temperature dependence of the resistivity to that of magnetic susceptibility for Np and Pu at the present time, but we have explained that the apparent contradiction between them might be irrelevant.

To conclude, we suggest some more experiments as a further check of our model:

(a) The resistivity of Pd and dilute *Pd*Ni alloys has been recently measured under pressure up to 4.5 kbar, but only at temperatures below 12 K[46]; such measurements should be extended to higher temperatures and pressures for Pd and Pd alloys.

(b) More experiments are certainly needed on the resistivity of α-cerium at normal or high pressures, to see if there is really a departure from the T law at high temperatures; obviously this experiment is not very easy, because we need to be at sufficiently high pressures to have a wide temperature range for α-Ce and at sufficiently low pressures to have still a large exchange-enhancement effect.

(c) High-temperature measurements of the resistivities would be also very interesting in exchange-enhanced compounds like Ni_3Ga and Ni_3Al.[47]

(d) The actinide metals and compounds are very promising as spin-fluctuation systems. The resistivity and the magnetic susceptibility under pressure of the actinide metals and compounds listed in Table III would be obviously very interesting. The resistivity of americium is worth measuring since the magnetic susceptibility of americium is larger than that of neptunium and plutonium.[38]

(e) The temperature dependence of $\chi(q, \omega, T)$ has an influence on all the physical properties: thermal conductivity, Lorenz number, thermopower, specific heat, etc. From the saturation value at high temperatures of the Lorenz number,[48] one can infer at once that the paramagnon thermal conductivity should vary linearly with T at high temperatures. Unfortunately although the experiments[49] on Pu indicate that it increases indeed for increasing temperature at high temperatures, there is not sufficient agreement between the data to allow us to establish a quantitative comparison with the theory.

ACKNOWLEDGMENTS

We wish to thank Professor J. Friedel for pointing out to us the interest of the problem and for many valuable comments. We also acknowledge interesting discussions with Dr. M. B. Brodsky and we are grateful to him for providing us with some of his data prior to publication.

---

*Part of thesis to be presented by R. Jullien at the University of Paris, Orsay, France.

†Laboratoire associé au Centre National de la Recherche Scientifique.

[1]D. L. Mills and P. Lederer, J. Phys. Chem. Solids 27, 1805 (1966); A. I. Schindler and M. J. Rice, Phys. Rev. 164, 759 (1967); P. Lederer and D. L. Mills, Phys. Rev. 165, 837 (1968).

[2]A. B. Kaiser and S. Doniach, Int. J. Magn. 1, 11 (1970).

[3]A. J. Arko, M. B. Brodsky, and W. J. Nellis, Phys. Rev. B 5, 4564 (1972).

[4]B. R. Coles, Phys. Lett. 8, 243 (1964).

[5]M. P. Sarachik, Phys. Rev. 170, 679 (1968).

[6]J. W. Loram, R. J. White, and A. D. C. Grassie, Phys. Rev. B 5, 3659 (1972).

[7]J. W. Loram, G. Williams, and G. Swallow, Phys. Rev. B 3, 3060 (1971).

[8]F. C. C. Kao, M. E. Colp, and G. Williams, Phys. Rev. B 8, 1228 (1973).

[9]N. Rivier and V. Zlatič, J. Phys. F 2, L99 (1972).

[10]N. Rivier and M. J. Zuckermann, Phys. Rev. Lett. 21, 904 (1968).

[11]R. Jullien, M. T. Beal-Monod, and B. Coqblin, Phys. Rev. Lett. 30, 1057 (1973).

[12]A. I. Schindler, R. J. Smith, and E. I. Salkovitz, J. Phys. Chem. Solids 1, 39 (1956); and Naval Research Laboratory Report No. 4974 (1957) (unpublished); I. Epelboin and A. Vapaille, C. R. Acad. Sci. (Paris) 244, 314 (1957); G. K. White and S. B. Woods, Philos. Trans. R. Soc. Lond. A 251, 273 (1959); T. Ricker and E. Pflüger, Z. Metallk. 57, 39 (1966).

[13]See, for instance, Rosemount Engineering Co., Minneapolis, Minn. E. T. I. Bulletin No. 1181 (1966) (unpublished).

[14]M. Nicolas-Francillon and D. Jerome, Solid State Commun. 12, 523 (1973).

[15]H. Katzman and J. A. Mydosh, Phys. Rev. Lett. 29, 998 (1972).

[16]M. B. Brodsky and R. J. Friddle, Phys. Rev. B 7, 3255 (1973).

[17]A. J. T. Grimberg, C. J. Schinkel, and A. P. L. M. Zandee, Solid State Commun. 11, 1579 (1972); and A. J. T. Grimberg, thesis (University of Amsterdam, 1973) (unpublished).

[18]See, for instance, G. T. Meaden, *Electrical Resistance of Metals* (Heywood, London, 1966), and references therein.

[19]R. O. Elliott, C. E. Olsen, and S. E. Bronisz, Phys. Rev. Lett. 12, 276 (1964).

[20]T. A. Sandenaw and R. B. Gibney, J. Phys. Chem. Solids 6, 81 (1958).

[21]R. Smoluchouski, Phys. Rev. 125, 1577 (1962), and references therein.

[22]M. J. Mortimer (unpublished).

[23]C. E. Olsen and R. O. Elliott, Phys. Rev. 139, A437 (1965).

[24]R. O. Elliott, C. E. Olsen, and J. Louie, J. Phys. Chem. Solids 23, 1029 (1962).

[25]A. Lefort, thesis (University of Poitiers, France, 1972)

(unpublished).
[26]S. Doniach, in *Seventeenth Conference on Magnetism and Magnetic Materials* (1971), edited by C. D. Graham, Jr. and J. J. Rhyne (American Institute of Physics, New York, 1972); in *Electronic Structure and Related Properties of Actinides*, edited by J. Darby, Jr. and A. J. Freeman (Academic, New York, to be published).
[27]M. T. Beal-Monod, S. K. Ma, and D. R. Fredkin, Phys. Rev. Lett. 20, 929 (1968); H. Rawn, P. Pedroni, J. R. Thompson, and H. Meyer, J. Low. Temp. Phys. 2, 539 (1970).
[28]D. Jerome, M. Rieux, and J. Friedel, Adv. Phys. 23, 1061 (1971); R. Jullien and D. Jerome, J. Phys. Chem. Solids 32, 257 (1971).
[29]D. B. McWhan and T. M. Rice, Phys. Rev. Lett. 22, 887 (1969).
[30]R. Jullien, E. Galleani d'Agliano, and B. Coqblin, Phys. Rev. B 6, 2139 (1972).
[31]See, for example, J. R. Schrieffer, *Theory of Superconductivity* (Benjamin, New York, 1964).
[32]See, for example, P. Nozières and D. Pines, *The Theory of Quantum Liquids* (Benjamin, New York, 1966).
[33]T. Kasuya, Prog. Theor. Phys. 16, 58 (1956).
[34]P. G. de Gennes and J. Friedel, J. Phys. Chem. Solids 4, 71 (1958).
[35]I. S. Gradshteyn and I. M. Ryzhik, *Tables of Integrals, Series and Products* (Academic, New York, 1965).
[36]D. L. Mills, J. Phys. Chem. Solids 34, 679 (1973).
[37]B. Coqblin, in Proceedings of the Seventh Rare-earth Conference Coronado, Calif. (1968) (unpublished), p. 79; J. Phys. (Paris) Suppl. 32, 599 (1971), and references therein.
[38]M. B. Brodsky, in *Proceedings of the Conference on Rare-earths and Actinides*, Durham, N. C., 1971 (Institute of Physics, London 1972), p. 75.
[39]A. Blaise and J. M. Fournier, Solid State Commun. 10, 141 (1972).
[40]M. J. Mortimer and J. Adamson (unpublished).
[41]A. R. Harvey, M. B. Brodsky, and W. J. Nellis, Phys. Rev. B 7, 4137 (1973); W. J. Nellis and M. B. Brodsky, in *Seventh Conference on Magnetism and Magnetic Materials* (1971), edited by C. D. Grahm, Jr. and J. J. Rhyne (American Institute of Physics, New York, 1972).
[42]M. B. Brodsky, private communication and unpublished.
[43]W. J. Nellis, A. R. Harvey, and M. B. Brodsky, in Eighteenth Conference on Magnetism and Magnetic Materials, Denver, Colo. (1972), AIP Conf. Proc. (to be published).
[44]F. A. Otter, J. Appl. Phys. 27, 197 (1956).
[45]J. Friedel (private communication).
[46]R. A. Beyerlein and D. Lazarus, Phys. Rev. B 7, 511 (1973).
[47]J. H. J. Fluitman, thesis (University of Amsterdam, 1970) (unpublished); and J. H. J. Fluitman, R. Boom, P. F. de Chatel, C. J. Schinkel, J. L. L. Tilanus, and B. R. de Vries, J. Phys. F 3, 109 (1973).
[48]M. T. Beal-Monod and D. L. Mills (unpublished).
[49]R. O. A. Hall and J. A. Lee, in Proceedings of the Fourth International Conference on Plutonium and other Actinides, Santa Fe, N. M., 1970, edited by W. N. Miner (unpublished), p. 35, and references therein.